

# Cold dark matter models with high baryon content

Martin White,<sup>1</sup> Pedro T. P. Viana,<sup>2</sup> Andrew R. Liddle<sup>2</sup> and Douglas Scott<sup>3</sup>

<sup>1</sup>*Enrico Fermi Institute, University of Chicago, 5640 S. Ellis Ave, Chicago, Illinois 60637, U. S. A.*

<sup>2</sup>*Astronomy Centre, University of Sussex, Falmer, Brighton BN1 9QH, U. K.*

<sup>3</sup>*Department of Physics & Astronomy, 129-2219 Main Mall, University of British Columbia, Vancouver, B. C. V6T 1Z4, Canada*

18 August 2021

## ABSTRACT

Recent results have suggested that the density of baryons in the Universe,  $\Omega_B$ , is much more uncertain than previously thought, and may be significantly higher. We demonstrate that a higher  $\Omega_B$  increases the viability of critical-density cold dark matter (CDM) models. High baryon fraction offers the twin benefits of boosting the first peak in the microwave anisotropy power spectrum and of suppressing short-scale power in the matter power spectrum. These enable viable CDM models to have a larger Hubble constant than otherwise possible. We carry out a general exploration of high  $\Omega_B$  CDM models, varying the Hubble constant  $h$  and the spectral index  $n$ . We confront a variety of observational constraints and discuss specific predictions. Although some observational evidence may favour baryon fractions as high as 20 per cent, we find that values around 10 to 15 per cent provide a reasonable fit to a wide range of data. We suggest that models with  $\Omega_B$  in this range, with  $h \simeq 0.5$  and  $n \simeq 0.8$ , are currently the best critical-density CDM models.

**Key words:** large-scale structure of the Universe – cosmology: theory – dark matter

## 1 INTRODUCTION

There is presently greater uncertainty regarding the baryon density of the Universe than there has been for many years. The standard theory of big bang nucleosynthesis (BBN), developed over more than 40 years and applied extensively to local abundance data, has long been considered as fixing the baryon density to a satisfyingly high level of accuracy. A typical quoted value a few years ago was  $\Omega_B h^2 = 0.0125 \pm 0.0025$ , where the uncertainty is to be interpreted as something like 95 per cent confidence (Walker et al. 1991; Smith, Kawano & Malaney 1993). Here  $\Omega_B$  is the baryon density in units of the critical density, and  $h$  is the present Hubble parameter in units of  $100 \text{ km s}^{-1} \text{ Mpc}^{-1}$ . However, recently it has been acknowledged that there are a range of possible systematic uncertainties in determinations of the primordial abundances (Wilson & Rood 1994; Sasselov & Goldwirth 1995; Skillman, Terlevich & Garnet 1995; Scully et al. 1996), which have led to a broadening of the preferred interval, particularly towards the upper end. Recent quoted ranges, at 95 per cent confidence, include  $0.010 < \Omega_B h^2 < 0.022$  by Copi, Schramm & Turner (1995a,b), with a similar result by Turner et al. (1996), and  $0.0125 < \Omega_B h^2 < 0.0275$  by Hata et al. (1996). Kernan & Sarkar (1996) quote a 95 per cent confidence upper limit  $\Omega_B h^2 < 0.032$ , while an analysis by Krauss & Kernan (1995) has also suggested higher baryon densities, although without quoting a specific range.

Added to that, it is now becoming possible to measure element abundances at high redshift as well as locally, through absorption systems in the spectra of distant quasars. Results for deuterium have so far been inconclusive (Songaila et al. 1994; Carswell et al. 1994, 1996; Wampler et al. 1996; Rugers & Hogan 1996a,b; Tytler, Fan & Burles 1996; Burles & Tytler 1996), with some very high abundances reported (implying a low baryon density) and also some low ones. There may be some reason to favour the lower determinations, in that most of the likely systematic effects, such as interloper hydrogen clouds, bias the abundance estimates upwards. However, only determinations in a large number of separate systems will truly resolve the issue. The most recent determination giving a low deuterium abundance (Tytler, Fan & Burles 1996; Burles & Tytler 1996) yields the result  $\Omega_B h^2 = 0.024 \pm 0.002 \pm 0.002 \pm 0.001$ , with the  $1\sigma$  uncertainties being statistical, systematic, and theoretical respectively. This is still consistent with the more recent determinations using local abundances, while reinforcing the view that the baryon density may be higher than previously thought.

Within the conventional picture, the new deuterium results can only be made consistent with BBN if the primordial helium abundance  $Y_P$  has been underestimated;  $\Omega_B h^2 = 0.025\text{--}0.035$  corresponds to 25 per cent helium, rather than the usual 23–24 per cent. However, this seems to be entirely within the bounds of possibility (e.g. Olive & Steigman 1995; Sasselov & Goldwirth 1995; Burles & Tytler 1996), given

possible systematic effects. The low deuterium values also imply very little destruction of primordial deuterium, in order to be consistent with the interstellar medium values, which give a constraint around  $\Omega_B h^2 \leq 0.031$  (McCullough 1992; Linsky et al. 1995). Hence values of  $\Omega_B \gtrsim 0.15$  (assuming  $h \simeq 0.5$ ) begin to run into quite firm limits. However, it may also be possible to relax the nucleosynthesis bound on  $\Omega_B$  with new particle physics, an example being the decaying tau neutrino proposal of Gyuk & Turner (1994), or by allowing inhomogeneities in the baryon-to-photon ratio (see e.g. Mathews, Kajino & Orito 1996 and references therein).

The other salient observational issue is the question of the baryon fraction in clusters of galaxies (White et al. 1993b; White & Fabian 1995; Elbaz, Arnaud & Böhringer 1995; Markevitch et al. 1996), which consistently gives values which are high for a critical-density universe. For example, a recent compilation by White & Fabian (1995) gives

$$\frac{\Omega_B}{\Omega_0} = 0.14^{+0.08}_{-0.04} \left( \frac{h}{0.5} \right)^{-3/2} \quad (1)$$

again at the 95 per cent level. There does seem to be variation in this quantity for individual clusters, but it is still unclear whether this is due to systematic effects. Certainly some clusters appear to have a baryon fraction as high as 20 per cent (see e.g. Mushotzky 1995). At the moment there is no obviously reliable lower limit to the cluster baryon fraction, although the values adopted by Steigman & Felten (1995),  $\Omega_B/\Omega_0 \geq 0.2 (h/0.5)^{-3/2}$ , and by Evrard, Metzler & Navarro (1996),  $\Omega_B/\Omega_0 \geq 0.11 (h/0.5)^{-3/2}$ , are typical of the range. Assuming there has been no significant segregation of the baryons, and that there has been no serious systematic underestimation of the mass of galaxy clusters (see e.g. Gunn & Thomas 1995; Balland & Blanchard 1996), this is hard to reconcile with a critical-density universe, unless  $\Omega_B$  has a higher value than given by the canonical BBN numbers.

There are some additional considerations which may favour an increase in the baryon fraction, although they would not make strong arguments on their own. One example is that a higher value of  $\Omega_B$  may bring simulations of Lyman alpha absorption systems more in line with data (Hernquist et al. 1996; Katz et al. 1996; Miralde-Escudé et al. 1996). Another example is the apparently high baryonic mass fraction in the halo of our Galaxy, in the form of MA-CHOs (Alcock et al. 1996; Bennett et al. 1996b). And a third is that higher  $\Omega_B$  may help proto-galaxy disks be more self-gravitating, thereby alleviating a problem with over-concentration of baryons in simulations of galaxy formation (see e.g. Steinmetz 1996).

We are interested in the implications of these changing notions about  $\Omega_B$  for models of structure formation, and in particular for the cold dark matter (CDM) model (Peebles 1982; Blumenthal et al. 1984; Davis et al. 1985) in the case of a critical-density universe (see Davis et al. 1992a and Dodelson, Gates & Turner 1996 for recent reviews). We will argue that a factor of two increase in the predicted baryon content from its circa 1993 value has a far from insignificant effect on the viability of such models, and indeed that there exist models from this class which provide a reasonable fit to the current data. The bottom line will be that models which are selected to conform with a wide range of constraints have:

(1) moderately tilted initial conditions; (b)  $h \simeq 0.5$ ; and (c)  $\Omega_B$  centred around a value of say 12 per cent.

The outline of the paper is as follows. In the next section we give an overview of the situation regarding critical-density CDM models, and in the following Section define our terminology and motivate our choice of model parameters. We then compare these high  $\Omega_B$  models with the available data on structure formation and on the cosmic microwave background (CMB) in Sections 4 and 5 respectively. We conclude with a discussion of some of the strengths and weaknesses of these models and future key observations.

## 2 THE BIG PICTURE

In order to obtain a critical-density universe of sufficient age, it is necessary to choose a Hubble parameter not much greater than  $h = 0.5$  (for example, an age greater than 12 Gyr requires  $h < 0.55$ ). Similar values for  $h$  are also necessary if one is to obtain a satisfactory structure formation model (White et al. 1995b; Liddle et al. 1996b). Some recent observational analyses have lent support to such a low Hubble constant (Schaefer 1996; Tammann et al. 1996; Branch et al. 1996), and such values even remain marginally consistent with the Freedman et al. (1994) measurement of  $h = 0.80 \pm 0.17$ . With  $h$  around 0.5, the predicted age of the universe appears to be consistent with the ages of the oldest globular clusters (Bolte & Hogan 1995; Chaboyer et al. 1995, 1996; Jiminez et al. 1996). For this value of  $h$ , the old nucleosynthesis determinations would indicate a universe with about 5 per cent baryons, while the higher values favoured more recently would be more like 10 per cent. As we shall see, this increase is far from insignificant, and indeed could be regarded as a new ‘standard’ value\*. The cluster number, centred around 15 per cent and going up to above 20 per cent, suggests the possibility of an even higher value.

If one is determined to retain a critical-density universe, it is extremely interesting that there is now strong evidence, from a structure formation perspective, in favour of these higher  $\Omega_B$  values. The demonstration of why this makes such a difference is the principal goal of the present paper. The gist of the argument is as follows. It is well known that, despite the strong appeal of simplicity and physical motivation, the standard CDM model (sCDM), based on a scale-invariant initial spectrum ( $n = 1$ ), a Hubble constant  $h = 0.5$  and with 5 per cent baryons, is unable to fit all the observational data. This is largely because, when normalized to reproduce the microwave anisotropies detected by the Cosmic Background Explorer (COBE) satellite (Bennett et al. 1996a), the power spectrum has too much short-scale power. If one is to retain the CDM hypothesis, modifications are required, and two have received particular attention, the first being to reduce the Hubble parameter (Bartlett et al. 1995) and the second to tilt the spectrum of density perturbations (Vittorio, Matarresse & Lucchin 1988; Bond 1992; Liddle, Lyth & Sutherland 1992; Cen et al. 1992; Muciaccia et al. 1993; Polarski & Starobinsky 1992). The former has the drawback that it appears necessary to reduce  $h$  to

\* In fact, many  $N$ -body simulations and other CDM calculations of the 1980s adopted this round number as a working value, and it is still sometimes used in this context.

about 0.35 (Liddle et al. 1996b), which is lower than most researchers are willing to accept. The latter has the problem that if one tilts the spectrum sufficiently to remove the unwanted short-scale power in the matter spectrum, then the tilt is also enough to remove the peak from the CMB anisotropy spectrum (White et al. 1995b; White 1996).

A range of CMB data now implies the existence of a power-spectrum peak at sub-degree scales (Scott, Silk & White 1995; Kogut & Hinshaw 1996), which seems even more compelling with the recent Saskatoon-95 (SK95) observations (Netterfield et al. 1996). This means that purely tilting the spectrum, while retaining the other standard CDM parameters, is beginning to look untenable. The situation improves somewhat if one combines a smaller tilt with a more modest reduction in  $h$  (White et al. 1995b; Liddle et al. 1996b), but as we shall see this is apparently still not enough if the currently favoured peak height is confirmed by future experiments.

The most natural way to try to resolve this conflict, while staying within the CDM paradigm, is to raise the baryon fraction. This has twin benefits. Regarding the radiation power spectrum, the effect of the extra baryons is to enhance the first peak. With enough baryons, this can go a long way towards compensating for the loss of height introduced by the tilt (the tilt in turn being required if one is to prevent the required  $h$  being too small), and hence retain compatibility with the recent CMB observations. The second benefit is that the baryons themselves help suppress the short-scale power in the matter power spectrum, since unlike the CDM they are unable to collapse until after decoupling. This means that the correct power spectrum shape can be obtained for a larger Hubble parameter, or a more modest tilt (cf. White et al. 1995b).

Before embarking on our discussion of critical-density CDM models, let us comment on some of the alternatives. One can reduce the short-scale power by assuming that a component of the dark matter is hot (Shafi & Stecker 1984; Bonometto & Valdarnini 1984; Davis et al. 1992b; Taylor & Rowan-Robinson 1992; Klypin et al. 1994; Jing et al. 1994). At present this is a perfectly satisfactory solution (especially if a modest tilt is also allowed (Liddle & Lyth 1993b; Schaefer & Shafi 1994; Pogosyan & Starobinsky 1995; Liddle et al. 1996b)), but loses the simplicity of having only cold dark matter. Even more fanciful solutions exist, including decaying neutrinos (Bond & Efstathiou 1991; Dodelson, Gyuk & Turner 1994; White, Gelmini & Silk 1995a; McNally & Peacock 1995), broken power laws or double inflation (Turner et al. 1987; Göttlober, Mücke & Starobinsky 1994; Peter, Polarski & Starobinsky 1994; Kates et al. 1995), and an additional isocurvature component (Kawasaki, Sugiyama & Yanagida 1996; Stompor, Banday & Górski 1996). There is also the possibility that astrophysical processes could play a role in determining the power spectrum of galaxy fluctuations (Babul & White 1991; Efstathiou 1992; Bower et al. 1992; Lambas et al. 1993), although it is not at all clear that such effects will be significant.

A more fundamental change is to stay with CDM but abandon critical-density models, going instead to low density. Viable models of this type are possible both in open universes (Ratra & Peebles 1994; Górski et al. 1995; Liddle et al. 1996a; Yamamoto & Bunn 1996) and in flat universes with a cosmological constant (Peebles 1984; Turner et al.

1984; Kofman & Starobinsky 1985; Efstathiou, Sutherland & Maddox 1990; Sugimotohara & Suto 1991; Efstathiou, Bond & White 1992; Kofman, Gnedin & Bahcall 1993; Krauss & Turner 1995; Ostriker & Steinhardt 1995; Stompor, Górski & Banday 1995; Liddle et al. 1996c). This has been seen as the easiest way to make CDM models consistent with the observational constraints, as indicated by the large number of papers exploring this possibility. We note though that pressure has been exerted on both the open and flat cosmological constant dominated approaches recently. The combination of the SK95 (Netterfield et al. 1996) and CAT (Scott et al. 1996) CMB observations appears to fix the location of the acoustic peak at around  $\ell \simeq 200$ , suggesting a flat geometry rather than a hyperbolic one. Furthermore, the somewhat lower normalization of the four-year *COBE* data (Bennett et al. 1996a; Banday et al. 1996; Górski et al. 1996; Hinshaw et al. 1996; Wright et al. 1996) exacerbates the problem that low-density open universes have a low normalization. Meanwhile, measures of the deceleration parameter using Type Ia supernovae (Perlmutter et al. 1996) suggest a universe which is decelerating rather than accelerating, which for a flat universe requires  $\Omega_0 > 2/3$ , agreeing with the quasar lensing constraint (Kochanek 1996). In addition, types of observations which have historically favoured high density, such as velocity power spectrum measures (Dekel 1994; Strauss & Willick 1995; Zaroubi et al. 1996), redshift-space distortions (Cole, Fisher & Weinberg 1995; Taylor & Hamilton 1996), the properties of voids (Nusser & Dekel 1993; Dekel & Rees 1994), and the absence of a prominent break in the non-linear power spectrum (Klypin, Primack & Holtzman 1996), continue to do so.

So, although there are many alternative paths to explore, it seems to us premature to relinquish the aesthetic appeal of critical density CDM models. Within the context of this general paradigm, there remain a number of parameters to be honed by the data. The value of the baryon fraction was traditionally a fixed quantity, and also thought to be low enough that the cosmological effects would be relatively unimportant. This is no longer true if one allows for the higher values of  $\Omega_B$  which now seem more credible, and moreover such variations are now significant at the level of detail which current data can distinguish. Raising  $\Omega_B$  to 10 per cent or above makes a substantial difference, as we will now show.

### 3 THE DARK MATTER POWER SPECTRUM

The matter power spectrum in the CDM model is specified by two functions. The initial spectrum of perturbations is taken to be a power-law  $P_{\text{init}}(k) \propto k^n$ , where  $n$  is the slope. The case  $n = 1$  is the scale-invariant spectrum, and  $n \neq 1$  models are often referred to as ‘tilted’. Inflationary models typically give  $n$  around one, though the possible range covers all the region of interest for structure formation<sup>†</sup>. The transfer function  $T(k)$  measures the

<sup>†</sup> Inflationary models may also produce a spectrum of gravitational waves which can influence the *COBE* normalization; typically these make it more difficult to fit the data and we do not consider them here.

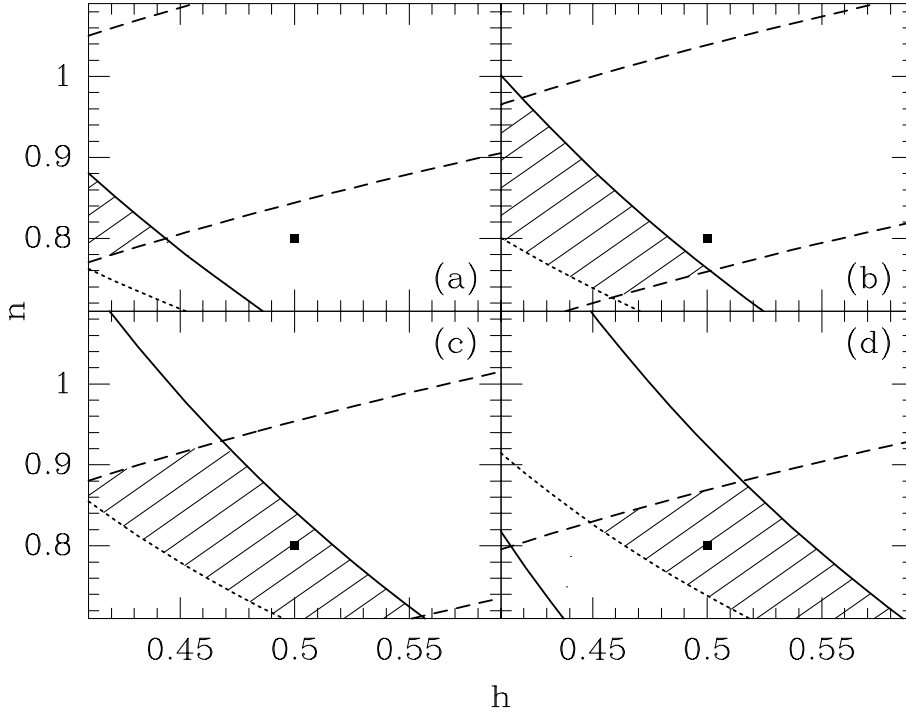


**Figure 1.** Linear theory constraint curves for CDM models in the  $h$ - $n$  plane for different values of  $\Omega_B h^2$ , namely (a) 0.0125, (b) 0.025, (c) 0.0375 and (d) 0.05. The squares indicate where the models in Table 1 lie. The curves and shaded areas show 95 per cent confidence regions from the galaxy correlation function (solid), the height of the CMB peak (dashed) and the abundance of damped Lyman alpha systems (dotted). It is the tension between these constraints which is eased by allowing a higher  $\Omega_B$ . Cluster abundance, quasar abundance and velocity information are less constraining than these. The shaded region is allowed by all data constraints, and some continuation above the dashed line would be permitted if reionization was sufficiently early.

amount of growth (relative to the infinite wavelength mode, and computed in linear theory) experienced by the modes of wavenumber  $k$ . The present linear power spectrum is given by  $P(k) \propto P_{\text{init}}(k) T^2(k)$ . In  $\Omega = 1$  CDM models, the transfer function is time-independent at late times; however, its form depends on the cosmological parameters  $h$  and  $\Omega_B$  describing the matter content of the Universe. Commonly, CDM models are described via a fit to the standard form<sup>‡</sup> of Bardeen et al. (1986)

$$T(q) = \frac{\ln(1 + 2.34q)}{2.34q} \times [1 + 3.89q + (16.1q)^2 + (5.46q)^3 + (6.71q)^4]^{-1/4}, \quad (2)$$

with  $q = k/h\Gamma$  (Sugiyama 1995; Hu & Sugiyama 1996). The parameter  $\Gamma$ , a function of both  $h$  and  $\Omega_B$  and referred to as the ‘shape parameter’, describes the shape of the matter transfer function. We have calculated transfer functions for our models numerically and then fit to this form.

In observational papers, the best-fitting model for a particular data set is often given in terms of an effective shape parameter,  $\Gamma_{\text{eff}}$ . This is usually done by fitting to the power

<sup>‡</sup> This form is not a good approximation at high  $\Omega_B/\Omega_0$  unless  $h \simeq 0.50$ . This could be important when considering low  $\Omega_0$  models should  $\Omega_B$  turn out to be 10 per cent or higher (Blumenthal, Dekel & Primack 1988).

spectrum under the assumption that  $n = 1$ . Since we will be allowing  $n$  different from unity, and also since the fit to the shape will depend on the range of scales considered, there is some ambiguity in the meaning of this  $\Gamma_{\text{eff}}$ , and so we will be explicit in our definition here. The ‘effective’ value of  $\Gamma$  for the theoretical models which we show in the table is obtained by finding the scale-invariant  $\Gamma$ -model which gives the same ratio of power on scales  $8h^{-1}\text{Mpc}$  and  $50h^{-1}\text{Mpc}$ , those scales being chosen as roughly the range typically probed by galaxy surveys. Since fitting a scale-invariant  $\Gamma$ -model to a tilted model is only approximate, it must be treated as only the roughest of guides and we shall always work from the true power spectrum.

Following Liddle & Lyth (1993a), the normalization can be specified by considering the value of the density fluctuation at horizon-crossing:  $\delta_{\text{H}}^2(k) \propto k^{n-1}$ . This is defined through the contribution to the rms fluctuation per logarithmic interval in wavenumber  $k$  as

$$\Delta^2(k) \equiv \frac{k^3 P(k)}{2\pi^2} \equiv \left(\frac{k}{H_0}\right)^4 \delta_{\text{H}}^2(k) T^2(k), \quad (3)$$

which is dimensionless. The normalization can be specified by giving the value of  $\delta_{\text{H}}$  at the present Hubble scale. The four-year *COBE* normalization of tilted critical-density CDM models can be well represented by a fitting function

$$\delta_{\text{H}}(k = H_0) = (1.94 \pm 0.13) \times 10^{-5} \quad (4)$$

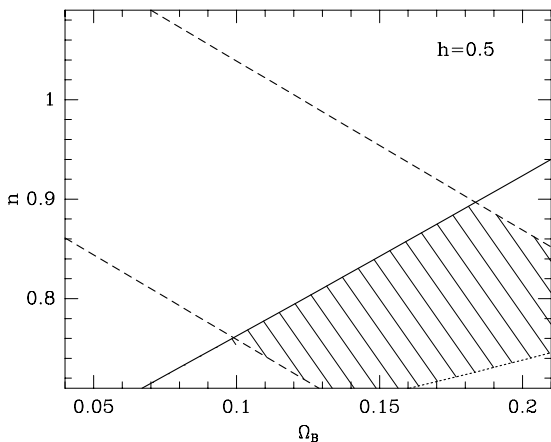


**Figure 2.** As Fig. 1, but in the  $\Omega_B$ - $n$  plane with  $h$  fixed at 0.50. The small region to the bottom right is ruled out because it has insufficient power to produce damped Lyman alpha systems at  $z = 4$ . The continuation of the shaded region upwards across the dashed line would be permitted by early reionization.

$$\exp[-0.95(n-1) - 0.169(n-1)^2],$$

which is accurate to better than 3 per cent for  $0.7 < n < 1.2$  (Bunn & White 1996). The effects of  $\Omega_B$  and  $h$  on this fit are negligible.

A quantity related to the power spectrum is the variance of the density field smoothed on a scale  $R$ , which is simply the integral of  $\Delta^2$ ,

$$\sigma^2(R) = \int \frac{dk}{k} \Delta^2(k) W^2(kR), \quad (5)$$

where we take the smoothing function  $W(kR)$  to be a spherical top-hat, given by

$$W(kR) = 3 \left( \frac{\sin(kR)}{(kR)^3} - \frac{\cos(kR)}{(kR)^2} \right). \quad (6)$$

Ways of comparing models with large-scale structure data are well developed in the literature. We use observations as described in Liddle et al. (1996b,c) to outline the preferred regions of parameter space (see also Silk 1994; Bond 1994; Bahcall 1995; White et al. 1995b; Primack 1996). Four crucial types of data turn out to be the most constraining, namely: the *COBE* observations of large-angle anisotropies; a compilation of intermediate-scale microwave anisotropy data; the abundance of damped Lyman alpha systems seen in quasar absorption spectra; and the shape of the galaxy correlation function. We shall consider several other types of data in addition to these, which prove not to give firm additional constraints.

We shall describe all of these in more detail in the following sections. However, to guide our later discussion, we show the results of the linear theory comparison now. The three parameters we can vary are  $\Omega_B$ ,  $h$  and  $n$ . Fig. 1 shows cuts of the parameter space at different choices of constant  $\Omega_B h^2$ . In each case there is an allowed region, but for the old nucleosynthesis value of  $\Omega_B$ , shown in Fig. 1(a), agreement is available only for very low  $h$ . There is considerable pressure from direct measurement against reducing  $h$  below 0.5, and it is rapidly problematic for large-scale structure

	$\Omega_B$			
	0.05	0.10	0.15	0.20
$\Gamma$	0.44	0.41	0.39	0.36
$\Gamma_{\text{eff}}$	0.36	0.33	0.31	0.28
$\sigma_8$	$0.77 \pm 0.06$	$0.72 \pm 0.05$	$0.66 \pm 0.05$	$0.61 \pm 0.05$
$\sigma_1$	$2.8 \pm 0.2$	$2.5 \pm 0.2$	$2.3 \pm 0.2$	$2.0 \pm 0.2$
$\sigma_{0.2}$	$5.0 \pm 0.5$	$4.5 \pm 0.3$	$3.9 \pm 0.3$	$3.4 \pm 0.3$
$z_{\text{ri}}$	14	12	11	9
$\tau$	0.05	0.08	0.10	0.11

**Table 1.** Power spectrum measures for selected CDM models. The models have  $\Omega_0 = 1$ ,  $h = 0.5$ ,  $n = 0.8$ , with four values of  $\Omega_B$  as shown. The values of  $\Gamma$  come from fitting to numerical evaluations of the transfer function for  $10^{-3} \leq k \leq 1 h \text{Mpc}^{-1}$ . The values of  $\Gamma_{\text{eff}}$  are fits to the ratio of the dispersions  $\sigma_R$  at  $R = 50 h^{-1}$  and  $R = 8 h^{-1} \text{Mpc}$ . The errors on  $\sigma_R$  reflect the  $1\sigma$  uncertainty from the *COBE* four-year normalization. The estimates of the reionization redshift  $z_{\text{ri}}$  and optical depth  $\tau$  are highly uncertain.

to go much above it, whatever the baryon density. For this reason we also show, in Fig. 2, a parameter-space cut at the value  $h = 0.5$ . This highlights the importance of varying the baryon density, and in many ways this figure can be said to represent our main result. Only by raising the baryon density to 10 per cent and above can critical-density CDM models be viable at  $h = 0.5$ . Both the galaxy correlation function and the CMB peak height exert pressure in that direction.

In order to focus our discussion, we select some particular models for closer study. We choose to concentrate on  $h = 0.5$ , for which  $n = 0.8$  is around the optimal choice, although less tilt can be accommodated for lower values of  $h$ . Our main aim is to consider variations of  $\Omega_B$ , and so we pick four values, corresponding to: the old BBN number (5 per cent); a number consistent with the low deuterium measurements and more recent BBN calculations (10 per cent); the favoured number from the cluster baryon fraction (15 per cent), which is some way above even the highest standard nucleosynthesis upper limits; and an extreme example representing close to the top of the range of observed cluster baryon fractions (20 per cent). In Table 1 we show a summary of important quantities for models spanning this range, calculated primarily in linear theory by numerical evolution of the coupled fluid, Einstein and Boltzmann equations<sup>§</sup>. Here the quantity  $z_{\text{ri}}$  is the redshift of reionization; it is estimated using the techniques of Liddle & Lyth (1995), and is highly uncertain. The optical depth to Thomson scattering,

$$\tau = 0.035 \Omega_B h [(1 + z_{\text{ri}})^{3/2} - 1], \quad (7)$$

inherits this uncertainty, and measures the probability of microwave photons being re-scattered, assuming full ionization from  $z_{\text{ri}}$  to the present.

<sup>§</sup> In White et al. (1995b) the values for  $\sigma_1$  were obtained from extrapolating  $P(k)$  as a power law from  $8 h^{-1} \text{Mpc}$  down to  $1 h^{-1} \text{Mpc}$ . This neglects the curvature of the transfer function over this range of scales and over-estimates  $\sigma_1$ . We use the full transfer function here.

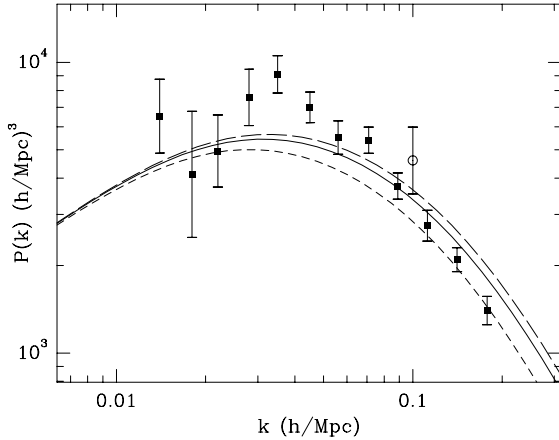


**Figure 3.** The matter power spectrum for  $\Omega_B = 0.05, 0.1, 0.2$ , the highest lines having the lowest baryon density (we omit the 15 per cent model for the sake of clarity). All models have  $h = 0.5$  and  $n = 0.8$ . The solid squares are taken from Peacock & Dodds (1994) with the 4 points at highest  $k$  omitted. We have adjusted the data to the best fit normalization for the  $\Omega_B = 0.1$  model. The open circle is the velocity-derived point from Kolatt & Dekel (1996); note however that the error bar shown on this point omits cosmic variance, which is large.

## 4 STRUCTURE FORMATION

We now discuss the main limits imposed on cosmological models from observations of the clustering properties of galaxies, the galaxy cluster abundance, peculiar velocities and high redshift object formation.

### 4.1 The galaxy correlation function

Perhaps the classic problem of standard CDM has been that the model has the wrong ‘shape’. Specifically the ratio of large-scale ( $\sim 50 h^{-1} \text{Mpc}$ ) power to small-scale ( $\sim 8 h^{-1} \text{Mpc}$ ) power is too small compared to observations. Both tilt and small-scale damping from a high baryon fraction help address this.

The current situation regarding the data relating to shape is somewhat uncertain. If we compare our models to the compilation of Peacock & Dodds (1994), taking the error bars at face value, then we require  $\Omega_B \geq 0.1$  to provide sufficient large-scale power, as can be seen in Fig. 3. For the model with  $\Omega_B = 0.1$  and  $n = 0.8$ , a simple  $\chi^2$  fit to the Peacock & Dodds (1994) data points assuming Gaussian uncorrelated error bars and allowing the normalization to vary, shows the model is excluded at about 97 per cent confidence, if one drops the four shortest-scale points which may be affected by non-linear biasing (Peacock 1996). If all the points are included this model fits at the 95 per cent confidence level. The models with higher  $\Omega_B$  fare better, being allowed at better than the 95 per cent confidence level, even excluding the four shortest-scale points. A reasonable conclusion based on this constraint then is that critical-density CDM models (with  $h \simeq 0.5$  and  $n \simeq 0.8$ ) are allowed provided that  $\Omega_B$  is about 10 per cent or greater.

The Peacock & Dodds (1994) data are a compilation to which several adjustments and/or corrections have been

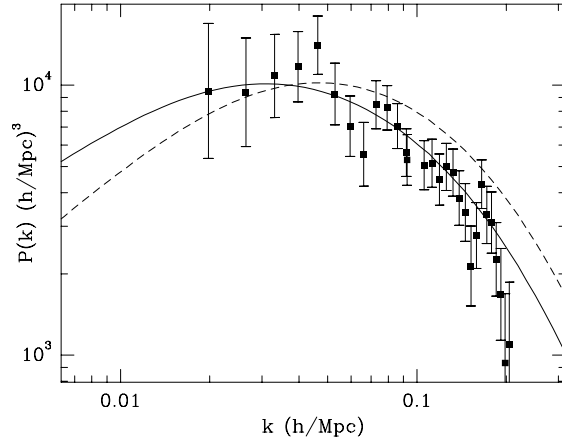


**Figure 4.** The redshift space matter power spectrum for the  $\Omega_B = 0.1$  model from Table 1 (solid line). The dashed line shows the result for standard CDM. The data are taken, without adjustment, from Tadros & Efstathiou (1995; weight 8000); approximately every second point is uncorrelated. This ignores a downward correction to the theoretical curves of roughly 15 per cent for  $k < 0.1 h \text{Mpc}^{-1}$ , arising from the window function of the surveys.

made. Since we have specific models in mind, we can carry the predictions forward to confront individual data-sets directly, rather than comparing to processed data. An example is shown in Fig. 4, where we compare the  $\Omega_B = 0.1$  model to the power spectrum of *IRAS* galaxies in redshift space, conveniently tabulated in Tadros & Efstathiou (1995). We have chosen this  $\Omega_B$  as the model which is only marginally allowed by Peacock & Dodds (1994). In this model the *IRAS* galaxies are almost unbiased tracers of the mass – we have not scaled the theory or the data points in Fig. 4 in any way. Specifically, we have assumed a redshift-space distortion parameter  $\beta = 1$ , and a small-scale exponential velocity distribution with  $\sigma = 280 \text{ km s}^{-1}$  to convert from real to redshift space (Cole et al. 1995). It is clear from Fig. 4 that this model fares extremely well against this survey, though it is less constraining than that of Peacock & Dodds (1994) since it incorporates less data.

The first firm indication that standard CDM lacked power on large scales came from the APM survey (Maddox et al. 1990; Maddox, Efstathiou & Sutherland 1996). To compare to this survey, we show in Fig. 5 the predicted angular correlation function  $w(\theta)$  for our four models. We use the fit in Jain, Mo & White (1995) to obtain the non-linear power spectrum; this is particularly important on scales less than  $1^\circ$ , but also has a modest effect at larger angles where it suppresses the correlation slightly. All our models clearly have sufficient large-scale power to fit this data, in contrast to the standard CDM model.

### 4.2 Galaxy cluster abundance

The present abundance of galaxy clusters requires  $\sigma_8 \simeq 0.6$ , with most authors agreeing fairly well on the central value but with differing opinions as to the uncertainty (Evrard 1989; Henry & Arnaud 1991; Bahcall & Cen 1993; White

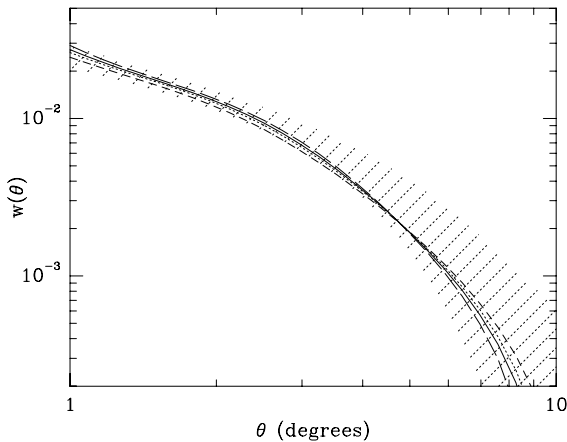


**Figure 5.** The galaxy angular correlation function  $w(\theta)$  for the APM survey as predicted by our models with  $h = 0.5$ ,  $n = 0.8$  and  $\Omega_B = 0.05$  (long dashed),  $0.10$  (solid),  $0.15$  (dotted) and  $0.20$  (short dashed). All curves have been *COBE* normalized with bias chosen to agree with the data at  $\sim 1^\circ$ . They include a correction from the non-linear part of the power spectrum. The shaded region represents the  $2\sigma$  error band from a fit to the APM data (Baugh & Efstathiou 1994).

et al. 1993a; Bond & Myers 1996c; Viana & Liddle 1996; Eke, Cole & Frenk 1996). Many determinations do not permit values as high as our lowest-baryon model predicts (see Table 1), though Viana & Liddle (1996) quote +32 per cent and -24 per cent at 95 per cent confidence, among the most conservative, which does just allow it. However, things are much better for the models with a higher baryon content. We find that any model of the type considered in this paper satisfying both the *COBE* and the galaxy correlation data constraints automatically satisfies the cluster constraint as well.

### 4.3 Peculiar velocities

The galaxy peculiar velocity field can be recovered through the POTENT procedure (Bertschinger & Dekel 1989) from peculiar velocity catalogs, such as the Mark III catalogue. It can then be used to constrain the amplitude of the power spectrum either directly, through the spatial derivatives of the peculiar velocity field (Dekel 1994; Strauss & Willick 1995), or indirectly, by means of the bulk velocity (Kolatt & Dekel 1996). Because the latter is sensitive to larger scales, results obtained through both methods do not necessarily coincide. Due to the very large cosmic variance, resulting from the fact that only local measurements have been made from a random field, we find that neither method further constrains the available parameter space left by the other observations. However, for comparison, we show in Fig. 3 a point from the POTENT velocity power spectrum of Kolatt & Dekel (1996). Notice that our models fit this well even without adding the cosmic variance. We note in passing that the velocity data can also be used to constrain the shape of the power spectrum, though at the moment results are not as robust as those using galaxy correlation data. Zaroubi et al. (1996) seem to prefer a higher  $\Gamma_{\text{eff}}$ , between 0.35 and 0.55

when marginalized over  $\sigma_8$ , than the galaxy surveys, though the uncertainty is large.

In addition, the question of the small-scale ( $\sim 1 h^{-1}\text{Mpc}$ ) velocities should be addressed, i.e. is the velocity field cold enough? This problem has been discussed by many people (see White et al. 1995b for references) but a clean comparison with the data remains difficult. Following White et al. (1995b), we compute the second moment of the mass correlation function  $J_2(1 h^{-1}\text{Mpc})$ , which is related to the rms velocity on the same scale. We find a reduction in short-scale power, as measured by  $J_2(1 h^{-1}\text{Mpc})$ , by a factor of 4 to 5 for our  $\Omega_B \gtrsim 0.1$  models, compared with standard CDM. Although this is a significant reduction, it may still be too hot relative to that measured in redshift catalogues, though this may be subject to substantial cosmic variance. We believe that the situation regarding velocities on these scales will probably require careful comparison of  $N$ -body simulations with observational results, which is beyond the scope of this paper.

### 4.4 High-redshift object abundance

We are going to concentrate on three types of objects found at high redshifts: damped Lyman alpha system (DLAS), galaxies and quasars. We will also mention the situation regarding clusters at intermediate redshifts. The technique we use to compare observed abundances with the ones predicted by our models is the standard Press-Schechter (1974) calculation (see Liddle et al. 1996b for a discussion of our particular implementation).

#### 4.4.1 Damped Lyman alpha systems

The observations of DLAS by Storrie-Lombardi et al. (1995) imply that at redshift 4, the most constraining point, the amount of neutral hydrogen in bound objects is

$$\Omega_{\text{HI}} = (0.0011 \pm 0.0002) h^{-1}. \quad (8)$$

To obtain a conservative bound, we assume that all the hydrogen in DLAS is in the neutral state, and taking the  $2\sigma$  lower limit, we obtain a lower bound on the baryon density at that redshift,

$$\Omega_B(z=4) \geq 0.0007 h^{-1}. \quad (9)$$

In order to compare this limit with our models we need to make some further assumptions regarding the nature of the DLAS. To be conservative we assume that the DLAS at such a high redshift arise predominantly within filamentary structures, which seems to be supported by recent hydrodynamical simulations (Katz et al. 1996), and consequently we use the threshold value of  $\delta_c = 1.5$  in the Press-Schechter calculation (Monaco 1995). We also conservatively use the 95 per cent upper limit on the *COBE* normalization, though the models also fit well at the central normalization.

In Fig. 6 we show an estimate of the *baryon* density in objects with a mass in excess of  $M$  at redshift 4 for our models. There is little difference at high redshifts between the models with higher baryon fractions. These models would come under pressure were it shown that the observed systems correspond to substantially more massive objects than usually supposed. However, under the reasonable assumption that the DLAS correspond to objects of masses  $10^{10}$

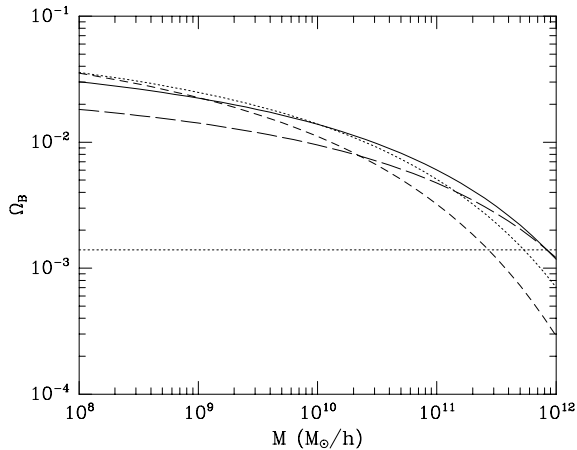


**Figure 6.** The *baryon* density in objects of mass greater than  $M$  at redshift 4, for our models. Along the right-hand side, the higher lines correspond to lower baryon density, the lines being 5 (long dashed), 10 (solid), 15 (dotted), and 20 (short dashed) per cent. The horizontal dotted line indicates the 95 per cent lower limit from DLAS observations (Storrie-Lombardi et al. 1995).

$h^{-1} M_{\odot}$  and greater, all of the models are comfortably allowed. We show the full parameter space constraints as the dotted curves in Figs. 1 and 2. The DLAS provide a limit on how much tilt can be introduced; at high baryon density this is presently a stronger constraint than the CMB peak height, as seen in Fig. 2.

#### 4.4.2 Lyman break galaxies

Recently Steidel and collaborators (Steidel et al. 1996a,b; Giavalisco, Steidel & Macchetto 1996) were able to detect galaxies between redshifts 3 and 3.5 using a technique based on the identification of the redshifted Lyman continuum break. Their results put a lower bound on the number density of Lyman break galaxies in that redshift range:

$$N_{\text{gal}}(z = 3.25) \geq 0.00288 h^3 \text{Mpc}^{-3}. \quad (10)$$

In Fig. 7 we plot the number density of collapsed objects with mass above  $M$  at redshift 3.25, for our four specific models. Here we use the threshold value of  $\delta_c = 1.6$  in the Press-Schechter calculation, which seems the optimal when the objects under consideration might have collapsed predominantly non-spherically due to local tidal fields (Monaco 1995; Bond & Myers 1996a,b). As before, we conservatively use the 95 per cent upper limit on the *COBE* normalization.

In order to constrain our models we need a rough estimate of the mass of the virialised halos with which the Lyman break galaxies are associated. According to the observations (Steidel et al. 1996b, Giavalisco et al. 1996) the luminosity of these galaxies arises predominantly within an approximately spherical central region with a radius of about  $2.5 h^{-1} \text{kpc}$ , where the velocity dispersion is between  $180$  to  $320 \text{ km s}^{-1}$ . Assuming that galaxy halos can be roughly approximated by a truncated singular isothermal sphere, these velocity dispersions correspond to halo masses in the region of  $5 \times 10^{11} h^{-1} M_{\odot}$  to  $3 \times 10^{12} h^{-1} M_{\odot}$ . However, the quoted interval for the velocity dispersion was obtained assuming

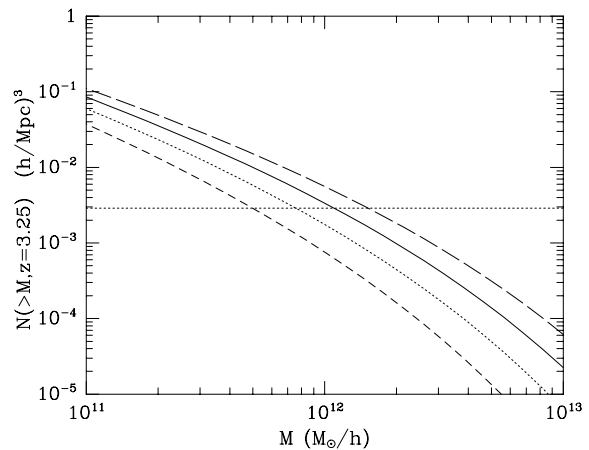


**Figure 7.** The number density of collapsed objects with mass above  $M$  for the four models at redshift 3.25. Higher lines correspond to lower baryon density, the lines being 5, 10, 15 and 20 per cent. The dotted line indicates the observed number density of Lyman break galaxies (Steidel et al. 1996a).

that the observed broadening of interstellar absorption lines is solely due to gravitational induced motions. If part of the broadening is due to non-gravitational effects, such as interstellar shocks arising from local star-forming regions, then the velocity dispersions would be smaller and hence also the derived halo masses. On the other hand, the true mean velocity dispersion of the halo is probably higher than the velocity dispersion of the stars, as these feel the effect of only the central part of the halo mass. In the future, spectra with higher signal to noise ratios and better resolution may enable the distinction between different sources of line broadening.

Another problem for our models may be the observation by Steidel et al. (1996a), using additional *K*-band photometry, that the Lyman break galaxies appear redder than one would expect if they were undergoing their first burst of star formation. However, there remains considerable uncertainty in estimating formation time from colours. Nevertheless, were it shown that these galaxies formed substantially earlier than the redshift at which they are observed, all models with critical density would be under severe strain.

#### 4.4.3 Quasars

For a long time, the abundance of quasars was the only information available about the process of structure formation at high redshifts. Now the abundances of DLAS, and more recently of Lyman break galaxies, probe similar epochs. Further, it has been shown that in general both DLAS abundances (see e.g. Liddle et al. 1996b) and Lyman break galaxies (Mo & Fukugita 1996) provide stronger constraints on theoretical models of structure formation than quasar abundances. The observed quasar number density at a redshift of 3.25 is about  $10^{-6} h^3 \text{Mpc}^{-3}$  (Schmidt, Schneider & Gunn 1995), and as can be seen in Fig. 7 this constraint is much weaker than that arising from the abundance of Lyman break galaxies; all models are viable for any quasar host galaxy mass up to  $10^{13} h^{-1} M_{\odot}$ . At even higher redshifts

the observed quasar number density does become more constraining, but not by much. For example, at redshift 4 our models are still able to reproduce the observed quasar number density, about  $3 \times 10^{-7} h^3 \text{Mpc}^{-3}$  (Schmidt et al. 1995), for any host galaxy mass up to  $10^{13} h^{-1} M_\odot$ , except the model with  $\Omega_B = 0.2$  which requires host galaxy masses from  $6 \times 10^{12} h^{-1} M_\odot$  upwards.

We also carried out a more careful analysis along the lines of Nusser & Silk (1993), allowing for relations between the abundance of quasars and their mean lifetime, and the luminosity and mean lifetime of a quasar and its minimum mass. We found that the conclusions given above hold for quasar mean lifetimes over a broad interval between about  $10^7$  and  $10^9$  yrs, the precise range depending on the fraction of collapsed halos hosting quasars, the amount of baryons in the halo used to form the central black hole and the quasar radiative efficiency. Our models and conclusions are similar to the tilted cases considered by Haehnelt (1993) and by Nusser & Silk (1993), who found that  $n \simeq 0.8$  models were allowed, although the quasars were then required to be radiating near to the Eddington limit and with lifetimes of  $\sim 10^7$  years. Note that for quasars, in common with other high- $z$  objects, there is a great degree of uncertainty in the estimation of the amount of collapsed matter at early times (see e.g. Katz et al. 1994; Eisenstein & Loeb 1995), and that it may be easier to form central black holes in higher  $\Omega_B$  models.

#### 4.4.4 Clusters

Finally, regarding intermediate redshift X-ray clusters, the best available observations at this moment are those of Lupino & Gioia (1995). Their sample of 6 clusters was selected from the *Einstein Observatory* Extended Medium Sensitivity Survey (EMSS). They have luminosities in excess of  $L_X = 1.25 \times 10^{44} h^{-2} \text{ergs s}^{-1}$  and redshifts between 0.55 and 0.83, where the most distant ever detected X-ray selected cluster is located. Given the comoving volume over which the survey was carried out, they conclude that the comoving number density of X-ray clusters with luminosities in excess of  $L_X$  is  $(8.8 \pm 3.44) \times 10^{-8} h^3 \text{Mpc}^{-3}$ , at a mean redshift of 0.66.

Again the difficulty is in obtaining a reliable mass estimate for these objects. However if we instead concentrate on the cluster X-ray temperatures, we can get a rough idea of what to expect from our models at  $z = 0.66$ . For that we first need to relate the X-ray luminosity  $L_X$  to an X-ray temperature. To a first approximation we can assume that the  $L - T$  relation at zero redshift also applies at  $z = 0.66$ . Following Henry et al. (1992), we translate  $L_X$  into a bolometric luminosity using  $L_{\text{bol}} = 1.18(kT)^{0.35} L_X$ , where  $kT$  is in keV. Using the observed zero redshift  $L - T$  relation given in David et al. (1993), and assuming  $h \simeq 0.5$ , we find that  $L_X$  corresponds to an X-ray temperature of roughly 6 keV. Following Viana & Liddle (1996), and using the values of  $\sigma_8$  in Table 1, we calculate the mass corresponding to these clusters under the constraint that their observed zero redshift number density be recovered (Henry & Arnaud 1991). We assume  $\delta_c = 1.6$  in the Press-Schechter calculation, integrate over temperature and obtain an estimate of the number density of X-ray clusters with  $L_{\text{bol}} > 1.1 \times 10^{45} h^{-2} \text{ergs s}^{-1}$  at  $z = 0.66$ . For our models with  $\Omega_B = 0.05$  and  $\Omega_B = 0.20$ , we

obtain  $4 \times 10^{\pm 1}$  and  $2 \times 10^{\pm 1} \times 10^{-8} h^3 \text{Mpc}^{-3}$  respectively, with the other models lying in between. Here the uncertainty, an order of magnitude in each direction, comes from pushing both the *COBE* normalization and the observed present number density of 6 keV X-ray clusters (Henry & Arnaud 1991) to their  $2\sigma$  confidence limits. As can be seen, all our models have mild difficulty in producing the observed number density of high-redshift clusters, but in view of the uncertainties there is still plenty of room for manoeuvre. However, current data may suggest that at fixed temperature the X-ray cluster luminosity is smaller at higher redshifts (e.g. Navarro, Frenk & White 1995); if this trend turns out to be correct, then *all* models with critical density will have great difficulty in reproducing the observed number density of high-redshift clusters.

## 5 COSMIC MICROWAVE BACKGROUND ANISOTROPIES

Any theory which purports to explain structure formation in the universe must fit both the large-scale structure data and the data on CMB anisotropies. The most influential piece of CMB data is the *COBE* normalization of large-scale structure theories (see White & Scott (1996) for a discussion and list of references); however, with the influx of data on smaller angular scales there are now extra constraints which must be met. For our purposes the strongest of these is that our model must be able to produce sufficient degree-scale power, which limits the amount to which we can tilt the primordial spectrum to alleviate the large-scale structure problems.

We show the radiation anisotropy power spectrum for our models, normalized to the *COBE* four-year data, in Fig. 8, along with a standard CDM model for comparison. The angular power spectrum is plotted in the usual way, with  $\ell(\ell + 1)C_\ell$  in dimensionless units. The index of the multipole expansion  $\ell \sim \theta^{-1}$ , with  $\theta$  in radians. We have chosen not to include any late reionization in these models, as the estimate of the reionization redshift is very uncertain. Including reionization would reduce the power on scales  $\ell \gtrsim 100$  by  $\exp(-2\tau)$ , where estimates of  $\tau$  are quoted in Table 1.

Notice that the increase in the baryon content has modulated the height of the peaks in the spectrum. The first and third peaks are increased in amplitude while the second peak is decreased. The tilt of the spectrum has monotonically decreased the power at small angular scales (high  $\ell$ ). This lack of power on smaller angular scales,  $\lesssim 15'$ , is a robust feature of our models which should be testable by the next generation of interferometers and array receivers.

Also shown in Fig. 8 is a selection of the current data on CMB anisotropies. From left to right the solid circles are: *COBE* (Hinshaw et al. 1996; 3 points, 1 upper limit), SP94 (Gundersen et al. 1995), MAX (Tanaka et al. 1996), Python (Ruhl et al. 1996, 3-beam), MSAM (Inman et al. 1996, 3-beam) and CAT (Scott et al. 1996, 2 points). The error bars are  $\pm 1\sigma$  while the horizontal lines indicate the range of angular scales to which the experiment is primarily sensitive. The solid squares indicate the SK95 data (Netterfield et al. 1996), with *no* allowance made for the 14 per cent calibration uncertainty. The upper limits are the highest- $\ell$  point from

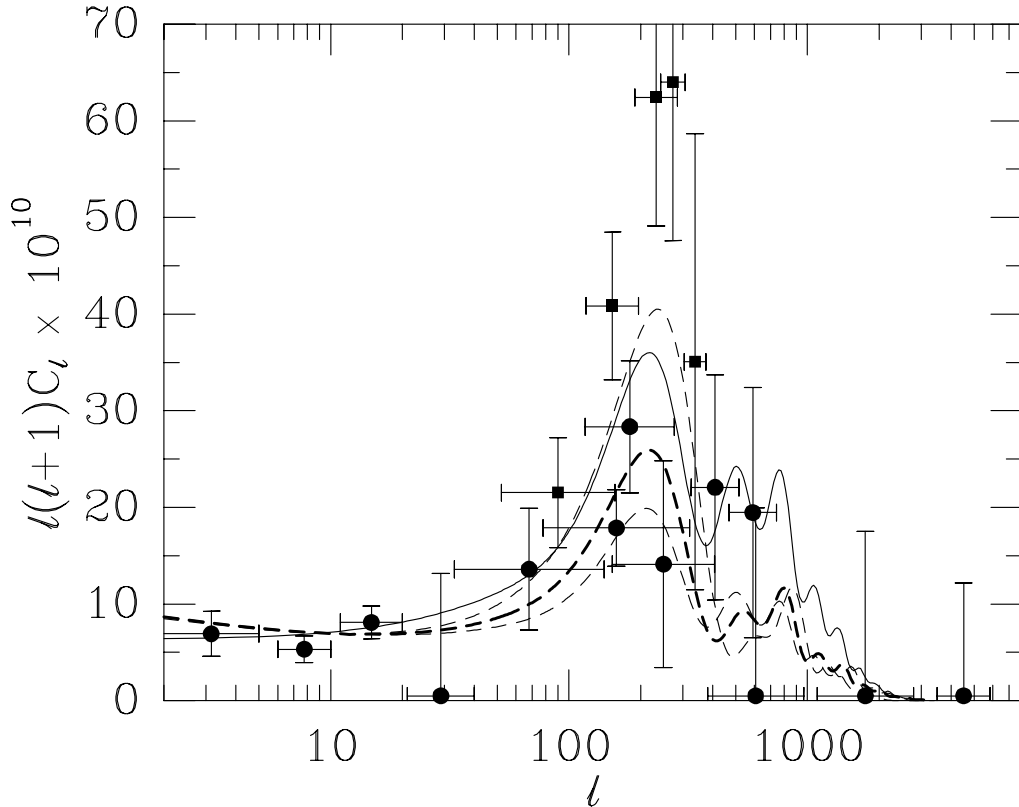


**Figure 8.** The radiation power spectrum for our models (dashed) with  $\Omega_0 = 1$ ,  $h = 0.5$  and  $n = 0.8$ . The curves have  $\Omega_B = 0.05, 0.1$  (thick) and  $0.2$  from bottom to top at  $\ell \sim 200$  (we have omitted the  $\Omega_B = 0.15$  line for clarity). The solid line is  $\Lambda$ CDM, with  $n = 1$ ,  $h = 0.5$  and 5 per cent baryons. All models have been normalized to the 4-year COBE data. The points are recent  $1\sigma$  detections and 95 per cent upper limits as discussed in the text. Solid circles from left to right are: COBE (3 points, 1 upper limit), SP94, MAX, Python, MSAM, CAT (2 points), White Dish, OVRO, ATCA. The solid squares are the SK95 points, without inclusion of the calibration uncertainty in the error bars. The error bars shown on this figure should be regarded as indicative only.

COBE at  $\ell \simeq 30$ , then at large  $\ell$  are White Dish (Tucker et al. 1993), OVRO (Readhead et al. 1989) and ATCA (Subrahmanyan et al. 1993), all quoted at 95 per cent confidence. For display purposes only, the points have been converted from temperature to power (temperature squared) with error bars  $\sigma_{T^2} = 2T\sigma_T$ .

These data have been selected from observations which have shown repeatability and which probe angular scales near the first peak. We have not included any allowance in the error bars for the effects of foreground subtraction. The expected or measured size of the foregrounds is discussed in the papers quoted above. Typically the experiments have mapped regions for which foreground contamination is known to be low and/or have used several frequencies to test for the presence of foregrounds. The subtraction or correction for foregrounds will generally weaken the lower limit on  $n$ . Where experiments have quoted two numbers from the same patch of sky we have chosen the highest  $\ell$ , which provides the largest lever arm. This is because such points are correlated in an unknown way. However, due to the observing geometry and data reduction strategy, the SK95 points are less than 20 per cent correlated (Netterfield et al. 1996), except for a common 14 per cent calibration

uncertainty, so we have included all 5 as uncorrelated. Corrections to this assumption should also permit a lower  $n$ .

To test the constraining power of the CMB data on our theory, we have computed the likelihood of fitting the data as a function of overall normalization  $\langle Q \rangle$ , tilt  $n$  and an additional multiplicative factor for the SK95 points to represent the calibration uncertainty. We have not tried to include the upper limits or the CAT points (which are correlated and have very large error bars). We show the likelihood in Fig. 9, marginalized over the normalization and SK95 calibration uncertainty. We have chosen a flat prior for  $\langle Q \rangle$ , which is anyway well determined by the COBE data. For the calibration uncertainty of SK95 we multiply by a Gaussian centred on unity with width 14 per cent (Netterfield et al. 1996). The calibration uncertainty from the other experiments was added in quadrature to the error bars on the points.

Our analysis here has not been very sophisticated, but it shows that while the tilted model with 5 per cent baryons does indeed have difficulty fitting the height of the peak (White et al. 1995b), models with 10 to 20 per cent baryons fare quite well. It would be interesting to perform a fit of these models to all of the data sets, rather than just the band-powers, to see how well they fare in detail. The best

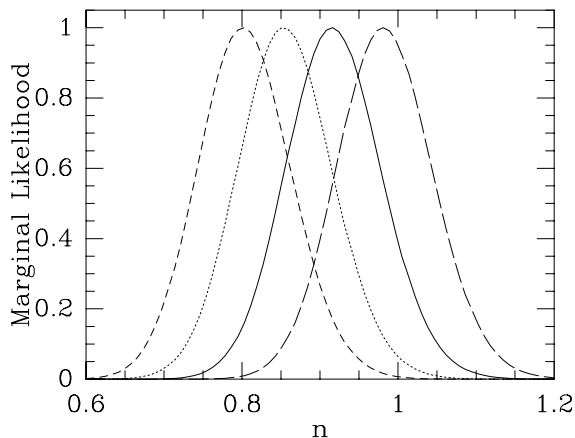


**Figure 9.** The marginal likelihood versus  $n$ , integrated over normalization and SK95 calibration, for a fit to a selection of the current CMB data. We show likelihoods (from right to left) for  $\Omega_B = 0.05, 0.1$  (solid),  $0.15$  and  $0.2$ . In all cases,  $h$  is fixed at  $0.50$ .

fitting  $n$  depends on the assumptions made about the tails of the SK95 calibration uncertainty since the fit of any model to the data becomes much better as the SK95 data are ‘lowered’. The  $\chi^2$  of the best-fitting model decreases by  $\sim 10$  if the SK95 calibration is decreased from 1 to 0.82 (consistent with the MSAM calibration) for example. With the SK95 calibration fixed at 1 the best-fitting model fits at about 95 per cent confidence level, this becomes 50 per cent if the calibration is fixed at 0.82. The first and second moments of the marginal likelihoods from Fig. 9 are  $n = 0.98 \pm 0.06, 0.92 \pm 0.06, 0.86 \pm 0.06$  and  $0.80 \pm 0.06$  for  $\Omega_B = 0.05, 0.10, 0.15$  and  $0.20$  respectively. If one includes the possibility of reionization, then the  $n = 0.8$  model with 10 per cent baryons begins to become unlikely. Including optical depth  $\tau$ , as given by Table 1, is approximately equivalent to shifting  $n \rightarrow n - 0.65\tau$ . Should observations further increase the preferred peak height, then the model with 10 per cent baryons will be disfavoured. On the other hand, if the height were to decrease, e.g. if some of the anisotropy were non-cosmological, even more tilt or reionization could be tolerated.

## 6 CONCLUSIONS

In this paper we have investigated the effects of assuming a baryon fraction two or more times higher than 1993 estimates of BBN would predict. With  $\Omega_B \gtrsim 0.1$  the baryons are becoming dynamically relevant, and so the increase has a non-negligible impact on the model of structure formation. We have concentrated on cold dark matter models with critical density, allowing  $\Omega_B h^2$  to vary within the range 0.0125 to 0.05.

Inclusion of a higher baryon fraction damps small-scale power in these models, since the growth in the baryons is suppressed by their interactions with the (relativistic) photons. More importantly, the higher baryon fraction allows one to tilt the initial spectrum by a greater amount before

coming into conflict with the growing evidence for enhanced power in the CMB on degree scales.

In order to facilitate more complete comparison of our model with data and to encourage numerical experiments, we have chosen a ‘preferred’ model with  $h = 0.5$ ,  $\Omega_B = 0.12$  and  $n = 0.8$ . This model is not the absolute best-fit when considering large-scale structure data alone, which would favour some combination of a slightly lower  $h$ , lower  $n$  or higher  $\Omega_B$ , as seen in Figs. 1 and 2. In selecting it, we have also paid heed to other evidence, such as nucleosynthesis and direct measurement of the Hubble constant, which suggest that one should avoid straying too far from the ‘standard’ values. Clearly changes in these values of  $\Omega_B$ ,  $h$  and  $n$  can play off against each other. Higher  $\Omega_B$  allows less tilt, and vice versa. If reionization occurs early, or if future CMB data require more power on degree scales, then this limits the tilt and thus the highest  $h$  which can be tolerated.

Several developments could falsify this model. Firstly we require that the Hubble constant be close to  $50 \text{ kms}^{-1} \text{ Mpc}^{-1}$ . Should it be higher than  $55 \text{ kms}^{-1} \text{ Mpc}^{-1}$ , it would be very difficult to fit the current data while retaining a critical matter density and pure CDM. A higher Hubble constant is in any case difficult for a critical-density universe since it predicts an age of below 12 Gyr. Of course, any firm measurement of the total density  $\Omega_0$  which obtained less than one would also rule this model out. In a similar vein, our model predicts  $\sigma_8$  to be in the interval from 0.5 to 0.8, and hence that *IRAS* galaxies are almost unbiased tracers of the mass. Both results ought to be refutable using future analyses of, respectively, velocity flows and redshift space distortions in galaxy surveys. Furthermore, the standard theory of big bang nucleosynthesis is only consistent with our assumed baryon fraction if the helium mass fraction  $Y_P$  has been underestimated. Should a firm upper limit on  $Y_P$  around 24.5 per cent be made then this model would require a violation of standard homogeneous nucleosynthesis by the introduction of extra physics at  $t \lesssim 3$  minutes. We also require the low deuterium determinations to be essentially correct, with the implication of little destruction of primordial deuterium.

There are several specific predictions which the high  $\Omega_B$  critical-density model makes. Starting with the theoretically cleanest of these, we predict that the radiation power spectrum will have reduced power, compared to standard CDM, at  $\ell \simeq 600$ , corresponding to angular scales  $\simeq 15'$ . This is seen clearly in Figure 8, and should be probed by the new generation of interferometer experiments CBI, VCA and VSA, and ultimately by the *MAP* and *COBRAS/SAMBA* satellites. On large scales, the shape of the matter power spectrum will differ from a scale-invariant  $\Gamma$ -model, due to the tilt in the initial spectrum of perturbations. Since our model has critical density, objects do not form as early as in open or cosmological constant dominated cosmologies, though the redshift of object formation is subject to large theoretical uncertainties. Finally, we predict a much higher fraction of dark baryons, though we are unable to say what form they will take. However, it is tempting to imagine that the halos of galaxies may have around a 20 per cent contribution from low-mass stars and other compact objects, as the recent results of the *MACHO* experiment indicate (Bennett et al. 1996b). We would certainly find it surprising if the *MACHO* fraction in galaxies was significantly less than the baryonic fraction in the Universe as a whole.

We briefly comment on the effect an increased baryon density would have on other structure-formation models. In all cases, the effect of the change to the CMB peak height is much more important than the change to the matter power spectrum. Recall that for critical-density CDM models, the main benefit is an increased CMB peak height, which is necessary to compensate for the need to tilt in order to get the galaxy correlations right. In low-density models, the spectral shape is already corrected by the changed value of  $\Omega_0 h$ , and so tilt is not required. However, observations only weakly constrain the tilt in such models, and so changing the baryon density will have a fairly neutral effect, offering neither advantages nor disadvantages — it simply moves the allowed region of parameters around a little. For high  $\Omega_B/\Omega_0$ , it may be possible to see oscillations in the matter power spectrum from the baryon component, but at critical density these are extremely small even in the 20 per cent model. For cold plus hot dark matter models on the other hand, a high baryon density could be threatening, because one must have less tilt in those models (the hot component having already adjusted the spectral shape) and hence there is the danger of too high a peak in the CMB. Early reionization might then be necessary to reduce it to acceptable levels.

Finally, let us end by noting that although critical-density CDM models remain viable, the present observational situation allows only a very limited range of parameters. If this paradigm is to be believed, then already the value of  $h$  is fixed at about the ten per cent level near 0.50, and similarly the slope  $n$  has to be around  $0.8 \pm 0.1$ .

## ACKNOWLEDGMENTS

MW is supported by the NSF and the DOE, PTPV by the PRAXIS XXI programme of JNICT (Portugal), ARL by the Royal Society and DS by NSERC (Canada). We thank Carlton Baugh, Marc Davis, Avery Meiksin, Joel Primack, Joe Silk, Rachel Somerville and Helen Tadros for discussions. ARL thanks Columbia University, Stanford University and Fermilab for hospitality while part of this work was carried out. PTPV acknowledges the use of the Starlink computer system at the University of Sussex.

## REFERENCES

- Alcock C. et al., 1996, *ApJ*, 461, 84  
 Babul A., White S. D. M., 1991, *MNRAS*, 253, 31P  
 Bahcall N. A., 1995, Princeton preprint, astro-ph/9503110  
 Bahcall N. A., Cen R., 1993, *ApJ*, 407, L49  
 Balland C., Blanchard A., 1996, Strasbourg preprint, astro-ph/9510130  
 Banday A. J., Górski K. M., Bennett C. L., Hinshaw G., Lineweaver C., Smoot G. F., Tenorio L., 1996, COBE preprint, astro-ph/9601065  
 Bardeen J. M., Bond J. R., Kaiser N., Szalay A. S., 1986, *ApJ*, 304, 15  
 Bartlett J. G., Blanchard A., Silk J., Turner M. S., 1995, *Science*, 267, 980  
 Baugh C. M., Efstathiou G., 1994, *MNRAS*, 267, 323  
 Bennett C. L. et al., 1996a, *ApJ*, 464, L1  
 Bennett D. P. et al., 1996b, *Bull. American Astron. Soc.*, 187, #47.07  
 Bertschinger E., Dekel A., 1989, *ApJ*, 336, L5  
 Blumenthal G. R., Faber S. M., Primack J. R., Rees M. J., 1984, *Nat*, 311, 517  
 Blumenthal G. R., Dekel A., Primack J. R., 1988, *ApJ*, 326, 539  
 Bolte M., Hogan C. J., 1995, *Nat*, 376, 399  
 Bond J. R., 1992, in Bergeron J., ed., *Highlights in Astronomy Vol 9*, p381, Proc of the IAU Joint Discussion, Kluwer, Dordrecht  
 Bond J. R., 1994, in Padmanabhan T., ed., *Proceedings of the IUCAA Dedication Ceremonies*, John Wiley and Sons, New York  
 Bond J. R., Efstathiou G., 1991, *Phys. Lett.*, B265, 245  
 Bond J. R., Myers S., 1996a, *ApJS*, 103, 1  
 Bond J. R., Myers S., 1996b, *ApJS*, 103, 41  
 Bond J. R., Myers S., 1996c, *ApJS*, 103, 63  
 Bonometto S. A., Valdarnini R., 1984, *Phys. Lett.*, A103, 369  
 Bower R. G., Coles P., Frenk C. S., White S. D. M., 1993, *ApJ*, 405, 403  
 Branch D., Fisher A., Baron E., Nugent P., 1996, Oklahoma preprint, astro-ph/9604006  
 Bunn E.F., White M., 1996, Berkeley preprint, astro-ph/9607060  
 Burles S., Tytler D., 1996, San Diego preprint, astro-ph/9603070  
 Carswell R. F., Rauch M., Weymann R. J., Cooke A. J., Webb J. K., 1994, *MNRAS*, 268, L1  
 Carswell R. F. et al., 1996, *MNRAS*, 278, 506  
 Cen R., Gnedin N. Y., Kofman L. A., Ostriker J. P., 1992, *ApJ*, 399, L11  
 Chaboyer B., Demarque P., Kernan P. J., Krauss L. M., 1995, *Science*, 271, 957  
 Chaboyer B., Demarque P., Kernan P. J., Krauss L. M., Sarajedini A., 1996, Case Western preprint, astro-ph/9604122  
 Cole S., Fisher K. B., Weinberg D. H., 1995, *MNRAS*, 275, 515  
 Copi C. J., Schramm D. N., Turner M. S., 1995a, *Science*, 267, 192  
 Copi C. J., Schramm D. N., Turner M. S., 1995b, *Phys. Rev. Lett.*, 75, 3981  
 David L. P., Spyz A., Jones C., Forman W., Vrtilik S. D., Arnaud K. A., 1993, *ApJ*, 412, 479  
 Davis M., Efstathiou G., Frenk C. S., White S. D. M., 1985, *ApJ*, 292, 371  
 Davis M., Efstathiou G., Frenk C. S., White S. D. M., 1992a, *Nat*, 356, 489  
 Davis M., Summers F., Schlegel D., 1992b, *Nat*, 359, 393  
 Dekel A., 1994, *ARA&A*, 32, 371  
 Dekel A., Rees M. J., 1994, *ApJ*, 422, L1  
 Dodelson S., Gyuk G., Turner M. S., 1994, *Phys. Rev. Lett.*, 72, 3754  
 Dodelson S., Gates E., Turner M. S., 1996, Fermilab preprint, astro-ph/9603081  
 Efstathiou G., 1992, *MNRAS*, 256, 43P  
 Efstathiou G., Sutherland W. J., Maddox S. J., 1990, *Nature*, 348, 705  
 Efstathiou G., Bond J. R., White S. D. M., 1992, *MNRAS*, 258, 1P  
 Eisenstein D. J., Loeb A., 1995, *ApJ*, 443, 11  
 Eke V. R., Cole S., Frenk C. S., 1996, *MNRAS*, 282, 263  
 Elbaz D., Arnaud M., Böhringer H., 1995, *A&A*, 293, 337  
 Evrard A. E., 1989, *ApJ*, 341, L71  
 Evrard A. E., Metzler C., Navarro J. F., 1996, *ApJ*, to appear, astro-ph/9510058  
 Freedman W. L. et al., 1994, *Nat*, 371, 757  
 Giavalisco M., Steidel C. C., Macchetto F. D., 1996, *ApJ*, to appear, astro-ph/9603062  
 Górski K. M., Ratra B., Sugiyama N., Banday A. J., 1995, *ApJ*, 444, L65  
 Górski K. M., Banday A. J., Bennett C. L., Hinshaw G., Kogut A., Smoot G. F., Wright E. L., 1996, *ApJ*, 464, L11  
 Göttlober S., Mücke J. P., Starobinsky A. A., 1994, *ApJ*, 434, 417  
 Gundersen J. O. et al., 1995, *ApJ*, 443, L57

- Gunn K. F., Thomas P. A., 1996, MNRAS, 281, 1133
- Gyuk G., Turner M. S., 1994, Phys. Rev. D, 50, 6130
- Haehnelt M. G., 1993, MNRAS, 265, 727
- Hata N., Scherrer R. J., Steigman G., Thomas D., Walker T. P., 1996, ApJ, 458, 637
- Henry J. P., Arnaud K. A., 1991, ApJ, 372, 410
- Henry J. P., Gioia I. M., Maccacaro T., Morris S. L., Stockke J. T., Wolter A., 1992, ApJ, 386, 408
- Hernquist L., Katz N., Weinberg D. H., Miralda-Escudé J., 1996, ApJ, 457, L51
- Hinshaw G., Banday A. J., Bennett C. L., Górski K. M., Kogut A., Smoot G. F., Wright E. L., 1996, ApJ, 464, L17
- Hu W., Sugiyama N., 1996, ApJ, to appear, astro-ph/9510117
- Inman C. A. et al., 1996, preprint, astro-ph/9603017
- Jain B., Mo H. J., White S. D. M., 1995, MNRAS, 276, 29
- Jiminez R., Thejll P., Jorgensen U., MacDonald J., Pagel B., 1996, MNRAS, to appear, astro-ph/9602132
- Jing Y. P., Mo H. J., Boerner G., Fang L.-Z., 1994, A&A, 284, 703
- Kates R., Müller V., Gottlöber S., Mückel J. P., Retzlaff J., 1995, MNRAS, 277, 1254
- Katz N., Quinn T., Bertschinger E., Gelb J. M., 1994, MNRAS, 270, L71
- Katz N., Weinberg D. H., Hernquist L., Miralde-Escudé J., 1996, ApJ, 457, L57
- Kawasaki M., Sugiyama N., Yanagida T., 1996, Tokyo preprint, astro-ph/9512368
- Kernan P. J., Sarkar S., 1996, Case Western preprint, astro-ph/9603045
- Klypin A., Holtzman J., Primack J. R., Regös E., 1994, ApJ, 416, 1
- Klypin A., Primack J., Holtzman J., 1996, ApJ, 466, 13
- Kochanek C. S., 1996, ApJ, 466, 638
- Kofman L., Starobinsky A. A., 1985, Sov. Astron. Lett., 11, 271
- Kofman L., Gnedin N. Y., Bahcall N. A., 1993, ApJ, 413, 1
- Kogut A., Hinshaw G., 1996, ApJ, 464, L39
- Kolatt T., Dekel A., 1996, Harvard preprint, astro-ph/9512132
- Krauss L. M., Kernan P., 1995, Phys. Lett. B, 347, 347
- Krauss L. M., Turner M. S., 1995, Gen. Rel. Grav., 27, 1137
- Lambas D. G., Abadi M. G., Nicotra M. A., Tissera P. B., 1993, ApJ, 414, 30
- Liddle A. R., Lyth D. H., 1993a, Phys. Rep., 231, 1
- Liddle A. R., Lyth D. H., 1993b, MNRAS, 265, 379
- Liddle A. R., Lyth D. H., 1995, MNRAS, 273, 1177
- Liddle A. R., Lyth D. H., Sutherland W., 1992, Phys. Lett., B279, 244
- Liddle A. R., Lyth D. H., Roberts D., Viana P. T. P., 1996a, MNRAS, 278, 644
- Liddle A. R., Lyth D. H., Schaefer R. K., Shafi Q., Viana P. T. P., 1996b, MNRAS, 281, 531
- Liddle A. R., Lyth D. H., Viana P. T. P., White M., 1996c, MNRAS, 282, 281
- Linsky J. L., Diplas A., Wood B. E., Brown A., Ayres T. R., Savage B. D., 1995, ApJ, 451, 335
- Luppino G. A., Gioia I. M., 1995, ApJ, 445, L77
- Maddox S. J., Efstathiou G., Sutherland W. J., Loveday J., 1990, MNRAS, 242, P43
- Maddox S. J., Efstathiou G., Sutherland W. J., 1996, Oxford preprint, astro-ph/9601103
- Markevitch R., Mushotzky R., Inoue H., Yamashita K., Furuzawa A., Tawara Y., 1996, ApJ, 456, 437
- Mathews G. J., Kajino T., Orito M., 1996, ApJ, 456, 98
- McCullough P. R., 1992, ApJ, 390, 213
- McNally S. J., Peacock J. A., 1995, MNRAS, 277, 143
- Miralde-Escudé J., Cen R., Ostriker J. P., Rauch M., 1996, ApJ, in press, astro-ph/9511013
- Mo H. J., Fukugita M., 1996, Max Planck preprint, astro-ph/9604034
- Monaco P., 1995, ApJ, 447, 23
- Muciaccia P. F., Mei S., de Gasperis G., Vittorio N., 1993, ApJ, 410, L61
- Mushotzky R., 1995, Goddard preprint
- Navarro J. F., Frenk C. S., White S. D. M., 1995, MNRAS, 275, 720
- Netterfield C. B., Devlin M. J., Jarosik N., Page L., Wollack E. J., 1996, ApJ, to appear, astro-ph/9601197
- Nusser A., Dekel A., 1993, ApJ, 405, 437
- Nusser A., Silk J., 1993, ApJ, 411, L1
- Olive K. A., Steigman G., 1995, ApJS, 97, 49
- Ostriker J. P., Steinhardt P. J., 1995, Nat, 377, 600
- Peacock J. A., 1996, Edinburgh preprint, astro-ph/9601135
- Peacock J. A., Dodds S. J., 1994, MNRAS, 267, 1020
- Peebles P. J. E., 1982, ApJ, 263, L1
- Peebles P. J. E., 1984, ApJ, 284, 439
- Perlmutter S. et al., 1996, Berkeley preprint, astro-ph/9602122
- Peter P., Polarski D., Starobinsky A. A., 1994, Phys. Rev. D, 50, 4827
- Pogosyan D. Yu., Starobinsky A. A., 1995, ApJ, 447, 465
- Polarski D., Starobinsky A. A., 1994, Nucl. Phys., B385, 623
- Press W. H., Schechter P., 1974, ApJ, 187, 452
- Primack J., 1996, Santa Cruz preprint, astro-ph/9604184
- Ratra B., Peebles P. J. E., 1994, ApJ, 432, L5
- Readhead A. C. S., Lawrence C. R., Myers S. T., Sargent W. L. W., Hardebeck H. E., Moffet A. T., 1989, ApJ, 346, 566
- Rugers M., Hogan C. J., 1996a, ApJ, 459, L1
- Rugers M., Hogan C. J., 1996b, AJ, 111, 2135
- Ruhl J., Dragovan M., Platt S.R., Kovac J., Novak G., 1996, Santa Barbara preprint, astro-ph/9508065
- Sasselov D., Goldwirth D. S., 1995, ApJ, 444, L5
- Schaefer B. E., 1996, ApJ, 460, L19
- Schaefer R. K., Shafi Q., 1994, Phys. Rev. D, 49, 4990
- Schmidt M., Schneider D. P., Gunn J. E., 1995, AJ, 110, 68
- Scott D., Silk J., White M., 1995, Science, 268, 829
- Scott P. F. S. et al., 1996, ApJ, 461, L1
- Scully S. T., Casse M., Olive K. A., Schramm D. N., Truran J., Vangioni-Flam E., 1996, ApJ, 462, 960
- Shafi Q., Stecker F. W., 1984, Phys. Rev. Lett., 53, 1292
- Silk J., 1994, Nucl. Phys. Supp., B35, 94
- Skillman E. D., Terlevich R., Garnett D. R., 1996, ApJ, to appear
- Smith M. S., Kawano L. H., Malaney R. A., 1993, ApJS, 85, 219
- Songaila A., Cowie L. L., Hogan C. J., Rugers M., 1994, Nat, 368, 599
- Steidel C. C., Giavalisco M., Pettini M., Dickinson M., Adelberger K. L., 1996a, ApJ, 462, L17
- Steidel C. C., Giavalisco M., Dickinson M., Adelberger K. L., 1996b, AJ, 112, 352
- Steigman G., Felten J. E., 1995, Spa. Sci. Rev., 74, 245
- Steinmetz, M., 1996, Max Planck preprint, astro-ph/9512013
- Stompor R., Górski K. M., Banday A. J., 1995, MNRAS, 277, 1225
- Stompor R., Banday A. J., Górski K. M., 1996, ApJ, 463, 8
- Storrie-Lombardi L. J., McMahon R. G., Irwin M. J., Hazard C., 1995, Cambridge preprint, astro-ph/9503089
- Strauss M., Willick J., 1995, Phys. Rep., 261, 271
- Subrahmanyan R., Ekers R. D., Sinclair M., Silk J., 1993 MNRAS, 263, 416
- Suginohara T., Suto Y., 1991, PASJ, 43, L17
- Sugiyama N., 1995, ApJS, 100, 281
- Tadros H., Efstathiou G., 1995, MNRAS, 276, L45
- Tammann G. A., Labhardt L., Federspiel M., Sandage A., Saha A., Macchetto F. D., Panagia N., 1996, Basel preprint, astro-ph/9603076
- Tanaka S. T. et al., 1996, Berkeley preprint, astro-ph/9512067
- Taylor A. N., Rowan-Robinson M., 1992, Nat, 359, 396
- Taylor A. N., Hamilton A., 1996, Edinburgh preprint, astro-ph/9604020

- Tucker G. S., Griffin G. S., Nguyen H. T., Peterson J. B., 1993, *ApJ*, 419, L45
- Turner M. S., Steigman G., Krauss L. M., 1984, *Phys. Rev. Lett.*, 52, 2090
- Turner M. S., Villumsen J. V., Vittorio N., Silk J., Juskiewicz R., 1987, *ApJ*, 323, 423
- Turner M. S., Truran J. W., Schramm D. N., Copi C. J., 1996, *ApJ*, 466, L59
- Tytler D., Fan X.-M., Burles S., 1996, *Nat*, 381, 207
- Viana P. T. P., Liddle A. R., 1996, *MNRAS*, 281, 323
- Vittorio N., Matarresse S., Lucchin F., 1988, *ApJ*, 328, 69
- Walker P. N., Steigman G., Schramm D. N., Olive K. A., Kang H.-S., 1991, *ApJ*, 376, 51
- Wampler E. J., Williger G. M., Baldwin J. A., Carswell R. F., Hazard C., McMahon R. G., 1996, *A&A*, to appear, *astro-ph/9512084*
- White D. A., Fabian A. C., 1995, *MNRAS*, 273, 72
- White M., 1996, *Phys. Rev. D* 53, 3011
- White M., Scott D., 1996, *Comm. Astrophys.*, 18, 289, *astro-ph/9601170*
- White M., Gelmini G., Silk J., 1995a, *Phys. Rev. D*, 51, 2669
- White M., Scott D., Silk J., Davis M., 1995b, *MNRAS*, 276, L69
- White S. D. M., Efstathiou G., Frenk C. S., 1993a, *MNRAS*, 262, 1023
- White S.D.M., Navarro J. F., Evrard A. E., Frenk C. S., 1993b, *Nat*, 366, 429
- Wilson T. L., Rood R. T., 1994, *ARA&A*, 32, 191
- Wright E. L., Bennett C. L., Górski K. M., Hinshaw G., Smoot G. F., 1996, *ApJ*, 464, L21
- Yamamoto, K. Bunn E. F., 1996, *ApJ*, 464, 8
- Zaroubi S., Dekel A., Hoffman Y., Kolatt T., 1996, Berkeley preprint, *astro-ph/9603068*

This paper has been produced using the Royal Astronomical Society/Blackwell Science  $\text{\LaTeX}$  style file.